Comparison of Power-Efficiency of Asthmatic Wheezing Wearable Sensor Architectures

Dinko Oletic(✉) and Vedran Bilas

Faculty of Electrical Engineering and Computing,
University of Zagreb, Unska 3, 10000 Zagreb, Croatia
{dinko.oletic,vedran.bilas}@fer.hr
http://www.fer.unizg.hr/liss

Abstract. Power-requirements of a wireless wearable sensor for quantification of asthmatic wheezing in respiratory sounds, a typical symptom of chronic asthma, are analysed. Two converse sensor architectures are compared. One featuring processing-intensive on-board respiratory sound classification, and the other performing communication-intensive signal streaming, employing compressive sensing (CS) encoding for data-rate reduction, with signal reconstruction and classification performed on the peer mobile device. It is shown that lower total sensor power, ranging from 216 to 357 µW, may be obtained on the sensor streaming the CS encoded signal, operating at the compression rate higher than 2x. Total power-budget of 328 to 428 µW is shown required in the architecture with on-board processing.

Keywords: m-health · Body sensor networks · Asthmatic wheeze detection · Digital signal processing · Compressed sensing · Power-analysis

1 Introduction

Asthma is one of the most widespread chronic respiratory disorders, requiring long-term treatment [1,2]. Quantification of its common symptom, occurrence of asthmatic wheezing in the respiratory sounds remains an open subject to research in the fields of pattern recognition [3–5], and biomedical sensor systems consisting of wearable sensors and smartphones (i.e. m-health) [6–9]. This paper builds upon previous research [10–15], and explores power-tradeoffs of asthmatic wheeze detection wireless wearable sensor architectures.

It is assumed that the sensor system consists of a body-worn sensor and a mobile device (i.e. smartphone). Sensor consists of the following subsystems: acoustic sensor, analog signal conditioning circuit, A/D converter, digital signal processing unit, and low-power radio for communication with smartphone [10]. Analysis covers three operating scenarios w.r.t. distribution of digitization, signal processing and communication among sensor system components.

In the first, (referent) operating scenario, sensor acquires the signal at Nyquist rate. Apart signal acquisition, no particular DSP processing tasks are

M. Magno et al. (Eds.): S-Cube 2016, LNICST 205, pp. 149–162, 2017.
DOI: 10.1007/978-3-319-61563-9_13

performed on sensor. Raw signal is wirelessly streamed over to the smartphone, where respiratory sound classification is performed. Scenario is motivated by the idea of simplification of the sensor design, and using the smartphone as the main signal processing platform.

In order to lower quantity of data (i.e. power) streamed from sensor to smartphone, second scenario utilizes concept of compressed sensing (CS) [16–18] to mutually lower the data rate, whilst retaining the low complexity of the sensor. Sensor performs signal acquisition at the sub-Nyquist rate [12], simultaneously compressing it (CS encoding). Compressed signal is streamed over to the smartphone. There, an additional decoder subsystem block performs signal reconstruction [13,14]. Finally, classification is performed [15].

In third scenario, sensor performs on-board (on-patient) signal acquisition and respiratory sound classification [11,15] (at Nyquist-rate), and periodically reports the classification outcome to smartphone. Scenario enables for highest sensor autonomy (independence of the radio link quality and smartphone processing resources), and minimizes data traffic [10].

Paper is organized as follows: In Sect. 2 each of sensor's subsystems is analysed from the aspect of power efficiency. Based on this, total sensor power consumption is analysed in Sect. 3. Paper is concluded in Sect. 4.

2 Power Analysis of Sensor Subsystems

2.1 Acoustic Sensors and Analog Signal Conditioning

Sensor and analog signal conditioning circuit design complying with standardised guidelines for respiratory sounds acquisition [19,20] was analysed. Microphones and accelerometers were evaluated as sensors. Representative sensor technologies were evaluated: electret-condenser microphone (KEEG1542, Knowles), MEMS microphone with analog output (ADMP404, Analog Devices; ICS-40310, Invensense), MEMS microphone with digital output (ADM441, Analog Devices). Capacitive MEMS accelerometers were evaluated (ADXL337/345, Analog).

Table 1 shows that in comparison to electret-condenser microphones and accelerometers, analog MEMS microphones feature highest power-efficiency, enabling for power consumption as low as 16 µW (i.e. ICS-40310). However, they feature high output impedance. Classically used electret-condenser microphones exhibit worst power-efficiency. Accelerometers offer comparable consumption to microphones, but may feature lower bandwidth and sensitivity. Advantage of digital systems-on-chips (SoC), such as ADMP441 or ADXL355 is integration of a complete signal chain, consisting of sensor, analog conditioning, ADC, and standard encoding of digitized output signal (I^2S or SPI).

Analog signal conditioning circuit for respiratory sound acquisition accommodates several functionalities: (1) signal amplification, as the typical sensor's output signal magnitudes reside in range of 1 to 10 mV (see typical sensitivities in Table 1). Amplifier's input is required to handle sensors output impedance typically in order of kΩ. (2) band-pass filtering with lower corner frequency around 100 Hz to filter-out heart sounds, and upper corner frequency adjusted

to sampling frequency for anti-aliasing. Assuming a microphone model chosen such to filter-out the low-frequencies by its frequency-characteristics, and that anti-aliasing is realised by passive RC filter, power consumption of an conditioning circuit based on a single instrumentation amplifier, such as INA333, was estimated at approx. 85 µW by Spice simulation.

Table 1. Comparison of acoustic sensors' power consumptions.

Technology	Component	Sensitivity	Imped	Power
MEMS mic., dig. (I^2S)	ADMP441	−26 dBFS	-	2520 µW @ 1.8 V
Electret cond. mic.	KEEG1542	−42 dB	2.2 kΩ	1000 µW @ 2.0 V
Analog accel.	ADXL337	300 mV/g	32 kΩ	900 µW @ 3.0 V
MEMS mic., analog	ADMP404	−38 dBV	200 Ω	375 µW @ 1.5 V
Accel., digital (SPI)	ADXL345	3.9 mg/LSB	-	350 µW @ 2.5 V
MEMS mic., analog	ICS-40310	−37 dBV	4.5 kΩ	16 µW @ 1.0 V

2.2 Signal Digitization

Two cases of signal digitization were analysed. First is Nyquist-rate signal sampling at 2 to 8 kHz [11] for scenarios of on-board processing or raw signal streaming), and second is compressive sampling (CS) at temporally non-uniform time-instants, as proposed in [12,14]. In case of CS, ADCs were tested at sub-Nyquist sampling rate corresponding to signal compression ratios of 2x to 8x (min. 250 Hz). Power efficiency tradeoffs of 12, 16, and 24 bit successive approximation (SAR) and sigma-delta analog to digital converters (ADCs) were compared. Components were chosen to support on-demand operating (triggered by signal processor), and entering power-saving state upon completing the conversion.

Table 2. Parameters of the tested ADCs

Technology	Component	ENOB	Nominal sample-rate	Average power @ 1 kSPS
12-bit SAR	ADS7924	11	10 kS/s	10 µW
16-bit SAR	AD7684	14	100 kS/s	15 µW
12-bit sigma-delta	ADS1014	12	3.3 kS/s	92 µW
16-bit sigma-delta	ADS1114	16	0.860 kS/s	368 µW
24-bit sigma-delta	ADS1251	19	20 kS/s	1.95 mW

A list of representative components with their respective performance is listed in Table 2. From power-up time, number of erroneous conversion samples, and conversion time, total active time was estimated for each component. From the

total active times, power consumptions at the nominal sampling rate, and the sleep powers, average powers of the active/sleep duty-cycle were extrapolated, for the whole analysed range of sampling frequencies from 250 Hz to 8 kHz.

Figure 1 confirms that the lowest power is obtained for ADC-s featuring a combination of lowest supply voltage, active and sleep current, and supporting high throughput. Specifically, for the required range of sample rates, SAR models show clear advantage in average power over sigma-delta. With the 24-bit sigma-delta, 1 mW suffices for the average sample rate of merely 500 Hz. Thus, 16-bit SAR is considered optimal for respiratory sound digitization, consuming in range of 6 to 123 µW for the range of sample rates of 250 Hz to 8 kHz. In comparison to 12-bit SARs, consumption of the 16-bit SAR is about 50% higher.

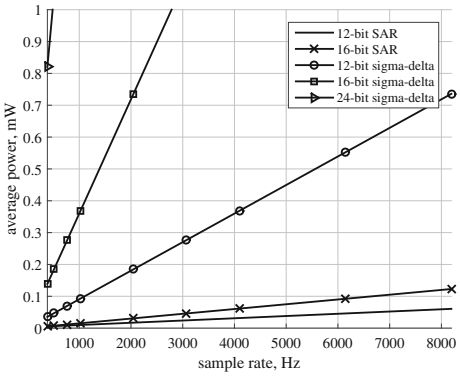

Fig. 1. Comparison of average power consumption of 12, 16 and 24-bit SAR and sigma delta ADCs in duty-cycle mode w.r.t sample rates of 250 Hz to 8 kHz.

2.3 Signal Processing

Processing Cores for Respiratory Sound Classification. Problem of asthmatic wheeze detection comes down to identification and spectro-temporal localization of unknown, temporally-changing instantaneous frequencies of individual frequency lines of asthmatic wheezing. Algorithms recently proposed for DSP implementation include either fast, heuristic algorithm [11] (i.e. referent), or more robust HMM-based [15] algorithms. Power-cost of their execution on commercial processing cores is analysed here. As a general rule, processing cores were selected to feature lowest active state power at highest operating frequency, in combination with low sleep state power, yielding potentially lowest average power [21]. Table 3 summarizes a list of the tested cores.

Three categories were analysed. First were the proprietary audio DSP cores, taking advantage of architectural accelerators for DSP functions, such as parallel multiply-and-accumulate units, barrel-shifters for floating-point operations, vector multiply, hardware FFT coprocessors, specific data transport I/O units

such as I^2S. Also they are typically supported with extensive library of software functions for audio processing. 16-bit fixed-point lowest-power DSP cores were evaluated for on-board signal processing: TMS320C5535 (Texas Instruments) and ADSP2188N (Analog Devices). They were compared to a legacy 16-bit 56xxx core MC56F8006 (Freescale Semiconductors), and higher powered 32-bit ColdFire core MCF51MM128 (Freescale Semiconductors).

Table 3. Parameters of the tested digital signal processors.

Processing core	Component	Freq., MHz	µW/MHz	Sleep, µW
audio DSP, 32-bit ColdFire	MCF51MM128	50	1740	84.0
audio DSP, 16-bit 56800E	MC56F8006	32	4282	521.4
audio DSP, 16-bit ADSP-21xx	ADSP2188N	80	562	180.0
audio DSP, 16-bit C55xx	TMS320C5535	100	220	220.0
high-perf. MCU, 32-bit ARM Cortex-M3	STM32L151C8	32	540	25.0
signal acq. MCU, 16-bit ARM 7 TDMI	ADUC7060	10	775	137.5
low-power MCU, 32-bit ARM Cortex-M0	LPC1102	50	462	6.6
low-power FRAM MCU, 16-bit MSP430	MSP430FR572x	24	275	19.2
Bluetooth SoC, 8-bit 8051	CC2541	32	628	2.7
Bluetooth SoC, 16-bit ARM Cortex-M0	nRF51422	32	495	6.9
Bluetooth SoC, 32-bit ARM Cortex-M4	BGM113	38.4	307	2.7
Bluetooth SoC, 32-bit ARM Cortex-M3	CC2640	48	110	4.9
Bluetooth SoC, 32-bit ARM Cortex-M4	nRF52832	64	100	1.7

Second category were general purpose MCU-s. High performance 32-bit ARM Cortex-M3 (STM32L151C8, ST Microelectronics) was compared to lower-powered ARM Cortex-M0 (LPC1102, Linear Technologies). 32-bit ARM cores were evaluated against proprietary 16-bit MSP430 core clocked at 2x lower frequency w.r.t. ARM Cortex-M0, but executing code from ultra-low power ferroelectric (FRAM) program memory (MSP430FR572x, Texas Instruments). Also, a dedicated signal acquisition controller based on older, 16-bit ARM 7 core coupled with high precision ADC, (ADUC7060, Analog Devices) was included.

Third category were processing cores embedded in system-on chip (SoC) Bluetooth 4 communication modules. Latest generation SoC featuring 32-bit

ARM Cortex-M3 (CC2640, Texas Instruments) is compared to two different ARM Cortex-M4 cores (nRF52832, Nordic Semiconductors; BGM113, Silicon Labs). They were compared to previous-generation SoCs featuring 16-bit ARM Cortex M0 (nRF51422, Nordic Semiconductors), and 8-bit 8051 core (CC2541, Texas Instruments).

Execution times of two analysed algorithms were derived from their respective analytical execution models given in [11,15]. Models show that algorithms' execution time is dominantly dependent on: (1) frequency resolution (number of observed frequency states M), and (2) number of frequency lines L. Motivated by the dependence of execution time on signal content, a test-environment was constructed to asses the dependency of average processing power to the symptoms severity, simulating the realistic operating conditions. Symptoms severity was modelled by: (1) percentage of respiratory cycle obstructed by wheezing (wheeze rate [2]), and (2) symptom occurrence frequency.

Execution time of both algorithms was calculated on each processing core for each combination of wheeze rate, symptom rate, number of processed frequency states (M). Cores' operating frequency, register width w.r.t. assumed 16-bit data width, and cost of multiplication w.r.t. addition were taken into consideration. Knowing the intervals between consecutive processing, processing duty-cycle (portion of active-time) was calculated from execution time. Finally, average processing power was calculated, using the active and sleep power. Sleep power was based on power-state where all required periphery for short wakeup, periodic signal sampling is operative, and the memory content is retained.

Example results, showing increase of average power proportional to symptoms rate and wheeze rate, for HMM-based algorithm are shown in Fig. 2, contrasting algorithm execution on two most representative cores: 100 MHz 16-bit audio processing DSP (C5535), and 48 MHz 32-bit general purpose ARM Cortex-M3 core within Bluetooth 4 SoC (CC2640). After normalization of clock frequencies, Cortex-M3 turns out 25% more efficient.

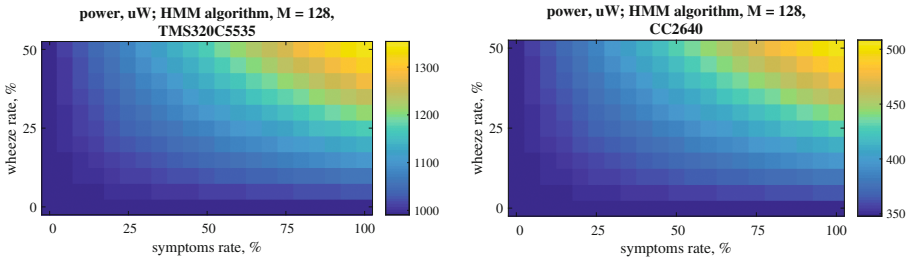

(a) 100 MHz audio DSP.

(b) 48 MHz ARM Cortex-M3.

Fig. 2. Power requirements on a 16-bit audio DSP and general purpose MCU.

Overall results are shown in Fig. 3. In Fig. 3a cores are sorted by worst-case power required for processing of wheezing w.r.t. power for processing of

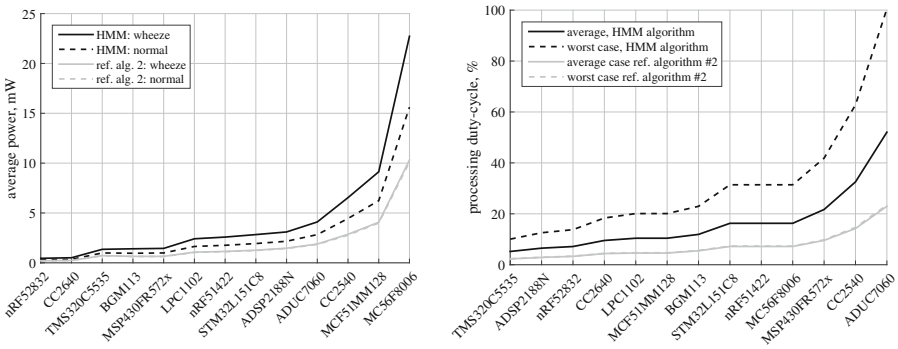

(a) Average-case processing power.

(b) Active-state duty-cycles.

Fig. 3. Ranking of processing cores by resources for wheeze classification.

normal respiratory sound, by both algorithms. It can be seen that for HMM-based algorithm, processing of wheezing may require approx. up to 45% more power than processing of normal respiratory sounds. On the other hand, referent algorithm shows negligible difference.

Best performance are obtained for ARM Cortex-M4 and M3 cores in Bluetooth 4 SoCs (nRF52832 and CC2640). Best overall results are obtained on a 64 MHz Cortex-M4 (nRF52832), ranging from 308 to 452 µW. Dedicated low-power audio C55xx DSP (TMS320C5535) requires approximately 2.7 times more average power. Worst efficiency is obtained with ADUC7060 signal acquisition controller, high-performance 32-bit ColdFire audio DSP core (MCF51-MM128), and the legacy 16-bit 568xx DSP core (MC56F8006). Also, legacy Bluetooth SoC module featuring 8051 core (CC2541) proves suboptimal due to 8-bit architecture, low clock-frequency etc.

Real-time processing constraints are analysed by examining average and worst-case processing duty-cycles, compared in Fig. 3b. Results show that least resources are spent by dedicated audio DSPs TMS320C5535 (worst-case 10% of processing time) and ADSP2188N. It is shown that due to low max. Clock-frequency (only 10 MHz), ADUC7060 signal-acquisition controller hardly meets worst-case real-time requirements when running HMM-based classification algorithm. Also, 8051 and MSP430 spend high portions of their processing time, 60% and 40%, respectively.

Processing Cores for CS Encoding. In the operating scenario of compressed signal streaming, power requirements of the CS signal encoder implementing sub-Nyquist sampling of analog input signal, at psudo-random, non-uniformly spaced sampling instants [12,14], are evaluated. As ADC power was covered in Sect. 2.2, analysis focuses on power spent on processing tasks implementing the LFSR pseudorandom number generator and the sampling period scheduler blocks in MCU software, and operation of the MCU's timer peripheral unit.

CS-encoding may be broken down to following tasks: (1) generation of LFSR pseudo-random output, (2) sampling-instant scheduling (3) timer setup of the timer, (4) triggering the ADC conversion. Cost of MCU implementation within FreeRTOS was empirically verified on prototype implementation on MSP430 to approx. 150 instructions per single CS-encoded sample.

Total cost of CS encoding was simulated for a range of CS sub-Nyquist sample rates corresponding to compression ratios of 2, 4, 5.33, and 8 w.r.t. Nyquist sampling frequency of 2 kHz. In addition to MSP430, power-cost of CS encoding was simulated on several additional MCU cores: on ADUC7060 signal acquisition controller, and on MCUs within Bluetooth 4 SoCs nRF52832, CC2640, BGM113, nRF51422 and CC2540. Results in Fig. 4 show that most efficient implementation may be achieved on Bluetooth 4 SoC ARM Cortex cores. On nRF52832 power for CS encoding ranges from 17 to 63 µW, while on CC2640 costs from 22 to 73 µW. It is shown that CS encoding on nRF52832 in worst simulated case spends less than 1% of processing time.

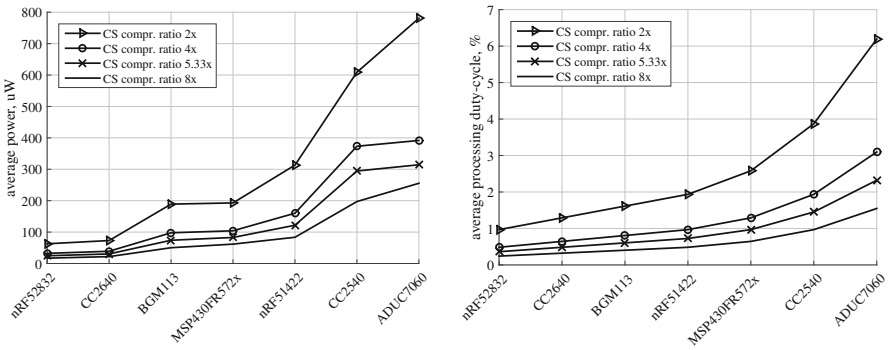

(a) Power for CS encoding.

(b) Proc. duty-cycle for CS encoding.

Fig. 4. Ranking of processing cores by resources for CS encoding.

2.4 Bluetooth Communication

Bluetooth 4.x (i.e. Smart, Low Energy) radio technology is evaluated for wireless data transfer, as it enables for interoperability with smarphones and medical certification [6], while retaining low-power operation. Highest level of integration is provided with system-on-chip (SoC) modules, packaging digital radio, radio controller implementing Bluetooth stack, an application processor, and a variety of standardized peripheral interfaces.

State-of-the-art Bluetooth 4 SoCs are analysed from stand point of power consumption: CC2640, CC2541 (Texas Instruments), BGM113 (Silicon Labs) and nRF52832 (Nordic Semiconductors). Table 4 compares their average power in most characteristic operating states: radio transmission (TX), radio listening (receiving, RX) and sleep. Power reduction in TX and RX of order of magnitude

of 2 to 3 times can be observed when comparing previous and actual generations of Bluetooth 4 SoCs (CC2541 w.r.t. CC2640, nRF52832, and BGM113). Increase of processing power enables for implementation of respiratory sound classification algorithms on-board SoC's application processor.

Bluetooth 4 communication protocol is designed to foster low average power by featuring intermittent, short active time (TX, RX) of the radio, in combination with long sleep time in between connection intervals. Data packets are exchanged only at predefined periodical *connection intervals*, during so-called *connection events*. Upon completion of the connection event, radio is put to sleep until the next one [22]. Duration of connection event is minimized by high throughput (typically 2 Mbit over-the-air). Typical waveform of the CC2640 radio's power-supply current measured during the connection event, segmented into a sequence of common power-states is shown in Fig. 5a (see labels 1 to 6).

Table 4. Parameters of the tested Bluetooth 4 SoC modules.

Component	Application processor	TX, mW	RX, mW	Sleep, µW
CC2541	8-bit 8051	36.4	35.8	2.0
BGM113	32-bit ARM Cortex-M4	16.3	16.1	2.6
nRF52832	32-bit ARM Cortex-M4	13.1	12.0	2.8
CC2640	32-bit ARM Cortex-M3	11.3	10.9	1.9

Due to number of parameters influencing durations of each power-state, we focused our power analysis on CC2640, on account of availability of extensive Bletooth power estimation guidelines, tools, and data [22]. Analysis assumes following parameteres and limitations of CC2640. Power is measured at supply voltage of 1.8 V. Output power of transmitter is set to 0 dBm as communication between sensor and smartphone is taking place at the very short range (i.e. <10 m). Maximal payload size during single connection event is limited by Bluetooth software stack to 256 bytes. Time between successive connection intervals may range from minimally 7.5 ms to maximally 4.0 s.

With given constraints, average power was calculated for each of three operating scenarios: (1) streaming of uncompressed data, digitized at Nyquist rate. Cases of sampling (streaming) rates of 8 kHz and 2 kHz are singled out. 8 kHz case corresponds to case where the referent crest-tracking algorithm [11] is employed for classification on smartphone. 2 kHz case corresponds to classification by HMM-based algorithm [15]. (2) in scenario of CS compressed signal streaming, 4 compression ratios w.r.t Nyquist frequency of 2 kHz were analysed: 2, 4, 5.33 and 8x. Payload size is calculated w.r.t. original signal block size of $N = 256$ and 75% overlap. Also, each TX payload size is increased by 2 additional bytes needed for pseudorandom seed. (3) scenario of respiratory sound classification on-board sensor. Here, binary block-wise classification outcome is encoded in periodically sent report messages. Connection period and payload size depend on classification algorithm (sampling frequency, signal block size),

and payload content: whether the stream of raw binary classification outcomes corresponding to each signal blocks is sent, or if wheeze-rate is calculated for a predefined temporal window. In all scenarios, 2-byte RX acknowledge message is assumed.

Relative contributions of the payload size and connection interval to average power were compared, by accumulating (buffering, storing) the TX data on sensor for multiple connection intervals spanning up to the maximal payload size, and then transmitting it in bulk. Table 5 summarizes tested scenarios, nominal payload sizes, and the span of possible connection intervals supporting the transmission given the payload size limitations (i.e. 256 bytes on CC2640).

Table 5. A list of tested communication scenarios, with best-case average power.

scenario, case	min. payload TX/RX, bytes	conn. intvl. span, ms	min. avrg. power, µW
Nyquist-rate streaming, f_s 8 kHz	256/2	16–32	914
Nyquist-rate streaming, f_s 2 kHz	128/2	31.25–62.5	373
CS streaming, compr. 2x	(64 + 2)/2	31.25–125	168
CS streaming, compr. 4x	(32 + 2)/2	31.25–250	81
CS streaming, compr. 5.33x	(24 + 2)/2	31.25–250	79
CS streaming, compr. 8x	(16 + 2)/2	31.25–250	77
class. result reporting	2/2	125–4000	8

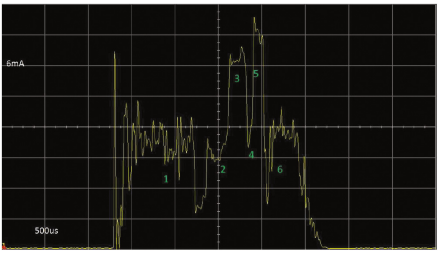

(a) Example waveform of current measured during a single Bletooth 4 connection event: 1 - RTOS wake-up, radio setup; 2 - radio on, transition to RX; 3 - radio listening (RX); 4 - transition from RX to TX; 5 - radio transmission (TX); 6 - processing the received packets, going to sleep [22].

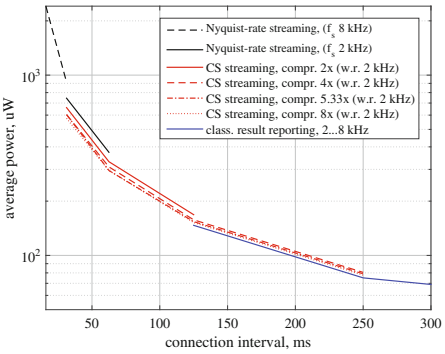

(b) Average power spent on Bluetooth 4 communication w.r.t. time between successive connection events.

Fig. 5. Power requirements of Bluetooth 4 communication.

Spans of average powers required for communication in each operating scenario w.r.t. time between successive Bluetooth connection events are shown in Fig. 5b.

It is shown that due to very short active times (i.e. high data rate), sleep power spent in-between connection intervals dominantly influences average communication power, much more than the change of payload size. This causes the average power to exponentially fall with increasing connection interval. Thus, it is proposed to maximally prolong (sleep) time between connection intervals by accumulating data, up to maximal transmission packet payload size.

Nyquist-rate data streaming proves most costly, costing 914 µW at 8 kHz (see Table 5). Drastic decrease in case of Nyquist-rate streaming at 2 kHz is primarily due to increase of connection intervals. Identical mechanism is the reason for decrease from 168 to 81 uW when step-up from CS compression ratio of 2x to 4x. On the other hand, minimal difference in average power is observed in the cases of identical connection intervals, where only payload size is increased (e.g. at the CS compression ratios 4x, 5.33x, and 8x). In scenario of on-board classification, minimal average power of only 8 µW is achieved at the maximal connection interval of 4 s.

3 Total Power Consumption

Here, total power of asthmatic wheeze sensor is analysed for each of three operating scenarios from Sect. 1. To enable for comparable performance in all operating scenarios, analysis is based on a sensor architecturally constituting of common subsystem components. As a sensor, analog MEMS microphone (such as ICS-40310) in combination with analog front-end from Sect. 2.1 is proposed. 16-bit SAR ADC (e.g. AD7684) is taken for digitalization. Processing and communication is implemented on the Bluetooth 4 SoC featuring the ARM Cortex-M4 processing core, proven optimal for both on-board classification and CS encoding tasks. In CS scenario, power-analysis is focused on compression ratios of 2x to 5.33x. Analysis is based on the representative CC2640 SoC.

Total powers are compared in Fig. 6. Being constantly powered and architecturally identical, the sensor and the analog conditioning circuit contribute equally to total power by 101 µW in all scenarios. Power contributions of remaining subsystems are scenario-dependent.

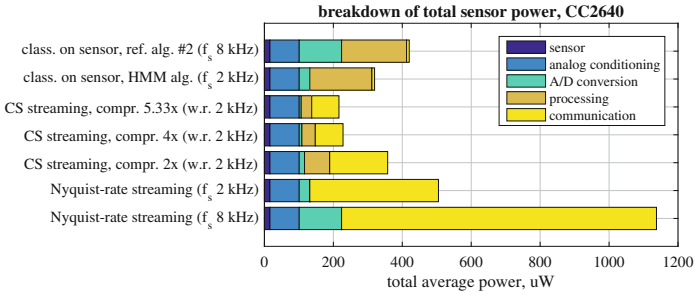

Fig. 6. Breakdown of total power per subsystems for different scenarios.

In the scenario of on-board classification, lower total power is obtained for the case of HMM-based algorithm operating on signal sampled at 2 kHz. Total power averaged 320 µW, with a major share of 56% being taken by classification algorithm. Classification using the referent crest-tracking algorithm results in 31% higher power (i.e. 420 µW).

In scenario of streaming of CS-encoded signal, total power scales down expectedly with increasing compression ratio. At the lowest compression ratios of 4x and 5.33x, it yields 228 and 216 µW, respectively. Majority of power is spent on communication. However, significant processing share related to CS encoding occurring at low compression ratios (e.g. 76 µW for compr. ratio of 2x) points to inefficiency of MCU software implementation of CS encoding. This could be improved by implementing CS encoder in hardware.

Scenario of uncompressed signal streaming virtually excludes any processing, and largest portion of power is spent on communication, proportional to the sample-rate. In best case (at 2 kHz, assuming classification using HMM-based algorithm on smartphone), power totalled 505 µW. At 8 kHz it doubled to 1138 µW. Thus, streaming of uncompressed signal proves to be the worst solution.

4 Conclusion

Architecture of the sensor for detection of asthmatic wheezing was analysed from the perspective of energy efficiency. Analysis has shown that analog MEMS microphones feature best power-efficiency, and with the proposed analog signal conditioning circuit total about 100 µW. For signal digitization, 16-bit successive approximation (SAR) ADC architecture proved optimal. Power analysis of wireless packet transfer via Bluetooth 4 has confirmed that power savings are more affected by connection intervals, than by payload size.

Lowest total power, ranging from 216 to 357 µW, may be obtained on the sensor performing CS encoding, operating at the compression rate higher than approx. 2x. By requiring less processing power, it outperforms best-case on-board classification 1.8 times. Also, by reducing the communication cost, it yields 2.2 times lower total power w.r.t. uncompressed signal streaming. This confirms usability of practically implemented CS encoding in systems where off-loading the sensor in terms of power consumption is a primary design criteria. CS offloads the communication subsystems on both peer devices, and shifts the most of the acquisition and processing power-burden from sensor to the processing on the smartphone (i.e. into the cost of CS reconstruction and respiratory sound classification). Efficiency of the MCU-based LFSR pseudorandom CS encoder design may be increased by hardware implementation.

In contrast, sensor design with on-board processing minimizes power spent on communication, and the bottleneck are respiratory sound classification algorithms. Power analysis of the processing subsystem has shown that 32-bit ARM Cortex M3/M4 cores embedded within Bluetooth 4 SoC modules feature optimal trade-off between performance and power consumption. Total power of 328 to 428 µW is observed.

References

1. Masoli, M., Fabian, D., Holt, S., Beasley, R.: Global Burden of Asthma. Medical Research Institute of New Zealand, Wellington (2010)
2. Boner, A.L., Piacentini, G.L., Peroni, D.G., Irving, C.S., Goldstein, D., Gavriely, N., Godfrey, S.: Children with nocturnal asthma wheeze intermittently during sleep. J. Asthma **47**(3), 290–294 (2010)
3. Hadjileontiadis, L.J.: Lung Sounds: An Advanced Signal Processing Perspective. Synthesis Lectures on Biomedical Engineering, vol. 9. Morgan & Claypool (2008)
4. Bahoura, M.: Pattern recognition methods applied to respiratory sounds classification into normal and wheeze classes. Comput. Biol. Med. **39**(9), 824–843 (2009)
5. Lozano, M., Fiz, J.A., Jané, R.: Automatic differentiation of normal and continuous adventitious respiratory sounds using ensemble empirical mode decomposition and instantaneous frequency. IEEE J. Biomed. Health Inform. **20**(2), 486–497 (2016)
6. Chen, M., Gonzalez, S., Vasilakos, A., Cao, H., Leung, V.C.: Body area networks: a survey. Mob. Netw. Appl. **16**, 171–193 (2011)
7. Lin, B.-S., Yen, T.-S.: An FGPA-based rapid wheezing detection system. Int. J, Environ. Res. Pub. Health **11**(2), 1573–1593 (2014)
8. Reyes, B.A., Reljin, N., Chon, K.H.: Tracheal sounds acquisition using smartphones. Sensors **14**(8), 13830–13850 (2014)
9. Boujelben, O., Bahoura, M.: FPGA implementation of an automatic wheezes detector based on MFCC and SVM. In: 2016 2nd International Conference on Advanced Technologies for Signal and Image Processing (ATSIP), pp. 647–650. IEEE (2016)
10. Oletic, D., Bilas, V.: Wireless sensor node for respiratory sounds monitoring. In: Anton, F. (ed.) IEEE I2MTC 2012, pp. 28–32. IEEE (2012)
11. Oletic, D., Arsenali, B., Bilas, V.: Low-power wearable respiratory sound sensing. Sensors **14**(4), 6535–6566 (2014)
12. Oletic, D., Skrapec, M., Bilas, V.: Prototype of respiratory sounds monitoring system based on compressive sampling. In: Zhang, Y.-T. (ed.) The International Conference on Health Informatics. IP, vol. 42, pp. 92–95. Springer, Cham (2014). doi:10.1007/978-3-319-03005-0_24
13. Oletic, D., Skrapec, M., Bilas, V.: Monitoring respiratory sounds: compressed sensing reconstruction via OMP on Android smartphone. In: Godara, B., Nikita, K.S. (eds.) MobiHealth 2012. LNICSSITE, vol. 61, pp. 114–121. Springer, Heidelberg (2013). doi:10.1007/978-3-642-37893-5_13
14. Oletic, D., Bilas, V.: Energy-efficient respiratory sounds sensing for personal mobile asthma monitoring. IEEE Sens. J. **16**(23), 1 (2016)
15. Oletic, D., Skrapec, M., Bilas, V.: Hidden Markov model in spectro-temporal tracking of asthmatic wheezing in respiratory sounds. In: Lacković, I., Vasic, D. (eds.) 6th European Conference of the International Federation for Medical and Biological Engineering. IP, vol. 45, pp. 5–8. Springer, Cham (2015). doi:10.1007/978-3-319-11128-5_2
16. Candès, E.J., Wakin, M.B.: An introduction to compressive sampling. Sig. Process. Mag. **25**(2), 21–30 (2008). IEEE
17. Kanoun, K., Mamaghanian, H., Khaled, N., Atienza, D.: A real-time compressed sensing-based personal electrocardiogram monitoring system. In: Design, Automation Test in Europe Conference Exhibition (DATE), pp. 1–6, March 2011
18. Bellasi, D.E., Benini, L.: Energy-efficiency analysis of analog and digital compressive sensing in wireless sensors. IEEE Trans. Circ. Syst. I: Regul. Pap. **62**(11), 2718–2729 (2015)

19. European respiratory review, 10 2000
20. Moussavi, Z.: Fundamentals of respiratory sounds and analysis. Synth. Lect. Biomed. Eng. **1**(1), 1–68 (2006)
21. Benini, L., de Micheli, G.: System-level power optimization: techniques and tools. ACM Trans. Des. Autom. Electron. Syst. **5**, 115–192 (2000)
22. Texas Instruments. Application report swra478a: measuring bluetooth smart power. Technical report, January 2016